NKFIH K 126065 final project report
University of Szeged, Szeged, Hungary
Report compiled by Ákos Kukovecz, kakos@chem.u-szeged.hu

## 1. Abstract

The current K 126065 project is the Hungarian implementation of the M-ERA.Net2 project "CLEARPV - Transparent perovskite solar cells". The CLEARPV project is realized in an international collaboration between the National Taiwan University, the company FrontMaterials Ltd (Taiwan), the TNO (Eindhoven) and the University of Szeged. It is important to realize that regardless of the title of the project, the actual tasks dedicated to the University of Szeged and financed by the K 126065 project are not about synthesizing perovskites or creating solar cells at this stage. Rather, the University of Szeged is responsible for developing and characterizing nanomaterials for use in the transfer layers of the cell.

## 2. Explanation of project acknowledgements

In the M-ERA.Net construction each partner is contracted by its own national funding agency. In Hungary, this is done through the National Research, Development and Innovation Office, who use their own project ID system. We are contractually obliged to acknowledge the support by using this national project ID and not the M-ERA.Net project acronym. The national project ID for implementing the CLEARPV project is K 126065. Therefore, all papers acknowledging this number should be counted as CLEARPV works.

## 3. Detailed activity report

### *3.1. Networking activities*

The Hungarian PI has participated at the kick-off event of the project in Eindhoven, the Netherlands in September 2017. He gave an overview of the Szeged facilities, discussed the realization of the M-ERA.Net2 project with the partners and participated in distributing the tasks within the network. As a result of this event, a Szeged PhD student (Levente Sánta) has established contact with a TNO researcher (Ilker Dogan). Several copper-oxide based nanostructures were synthesized and characterized at Szeged in this cooperation. In August 2018 these samples were sent to TNO for further testing as transfer layer materials.

A major networking activity within the consortium took place between March 2019 – May 2019, when Mr. Levente Sánta, a graduate student at the University of Szeged visited TNO in Eindhoven for joint research in photovoltaics. His travel and salary were covered by the University of Szeged, work infrastructure, materials and supervision were provided by TNO.

The Szeged node was active in organizing the CLEARPV mini-symposium of the SIWAN 2018 conference. SIWAN stands for Szeged International Workshop on Advances in Nanoscience. It is a biennial nanotechnology conference organized by the University of Szeged in even years. Although the conference itself will take place in the 2nd project year (7-10 October, 2018), all the organizing work was completed in the present reporting period. The CLEARPV symposium was co-organized by the CLEARPV node heads Prof. Wei-Fang Su and Prof. Yulia Galagan.

The Szeged node has purchased the web address https://www.clearpv.org and created the website for the CLEARPV project there.

*3.2. Research results*

**1) Balázs Buchholcz, Kamilla Plank, Miklós Mohai, Ákos Kukovecz, János Kiss, Imre Bertóti, Zoltán Kónya: Morphology Conserving High Efficiency Nitrogen Doping of Titanate Nanotubes by NH3 Plasma, *Topics in Catalysis*, 61 (2018) 1263-1273.**

Titanate nanotubes offer certain benefits like high specific surface area, anisotropic mesoporous structure and ease of synthesis over other nanostructured titania forms. However, their application in visible light driven photocatalysis is hindered by their wide band-gap, which can be remedied by, e.g., anionic doping. Here we report on a systematic study to insert nitro-gen into lattice positions in titanate nanotubes. The efficiency of N2+ bombardment, N2 plasma and NH3 plasma treatment was compared to that of NH3 gas synthesized in situ by the thermal decomposition of urea or NH4F. N2+ bombarded single crystalline rutile TiO2 was used as a doping benchmark (16 at.% N incorporated). Surface species were identified by diffuse reflectance infrared spectroscopy, structural features were characterized by scanning electron microscopy and powder X-ray diffraction measurements. The local chemical environment of nitrogen built into the nanotube samples was probed by X-ray photoelectron spectroscopy. Positively charged NH3 plasma treatment offered the best doping performance. This process succeeded in inserting 20 at.% N into nanotube lattice positions by replacing oxygen and forming Ti–N bonds. Remarkably, the nanotubular morphology and titanate crystal structure were both fully conserved during the process. Since plasma treatment is a readily scalable technology, the suggested method could be utilized in developing efficient visible light driven photocatalysts based on N-doped titanate nanotubes. It is also possible that the anisotropic, N-doped titanates will have relavance in the CLEARPV cell structure. (Buchholcz et al., Topics in Catalysis 2018).

**2) Tamás Varga, Ágnes Tímea Varga, Gergő Ballai, Henrik Haspel, Ákos Kukovecz, Zoltán Kónya: One step synthesis of chlorine-free Pt/Nitrogen-doped graphene composite for oxygen reduction reaction, *Carbon* 133 (2018) 90-100.**

Chlorine-free Platinum/nitrogen-doped graphene oxygen reduction reaction catalysts were synthesized by a one step method of annealing a mixture of platinum acetylacetonate and graphene oxide under ammonia atmosphere. Nanoparticles with close to the ideal particle size for oxygen reduction reaction (ORR) were formed, i.e., with diameter of 3–4 nm (500 and 600 °C) and 6 nm (700 °C). X-ray photo- electron spectroscopy confirmed the successful introduction of both pyridinic and pyrrolic type nitrogen moieties into the graphene layers, which indicates a strong interaction between the nanoparticles and the graphene layers. The electrocatalytic activity of glassy carbon electrodes (GCE) modified with the synthesized Pt/NG samples for oxygen reduction was compared to that of a platinum/carbon black catalyst modified electrode in acidic and alkaline media. Based on the measured limiting current den-sities and calculated electron transfer number, the highest activity was measured in acidic and alkaline media on the samples annealed at 600 and 700 °C, respectively. The figure below presents the mass transfer-corrected Tafel plots in the oxygen reduction reaction (ORR) for Pt/NG_500 °C, Pt/NG_600 °C, Pt/ NG_700 °C, and Pt/CB modified GCE in 0.1 M KOH.

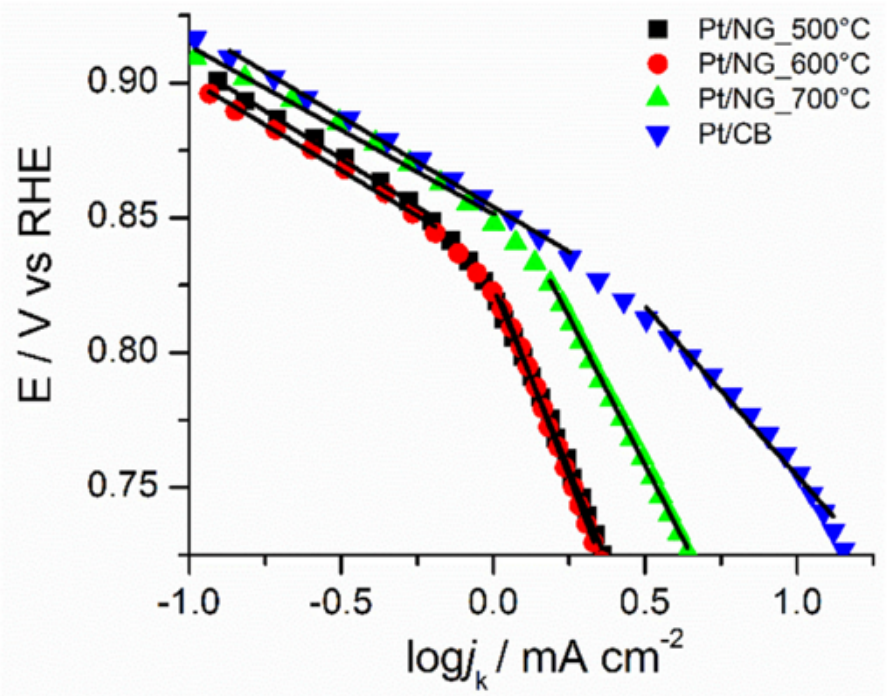


Linear sweep voltammograms of the GCE electrode modified with (a) Pt/CB catalyst and the Pt/NG composites, prepared at the temperatures indicated, are presented in the figure below. LSV curves were recorded at room temperature in O2 saturated 0.1M KOH solution at a scan rate of 10mVs$^{-1}$. Inset graphs show Koutecky-Levich plots for oxygen reduction recorded on surface modified GCEs. Electron transfer numbers were calculated from the fitted Koutecky-Levich equation. (T. Varga et al., Carbon 2018).

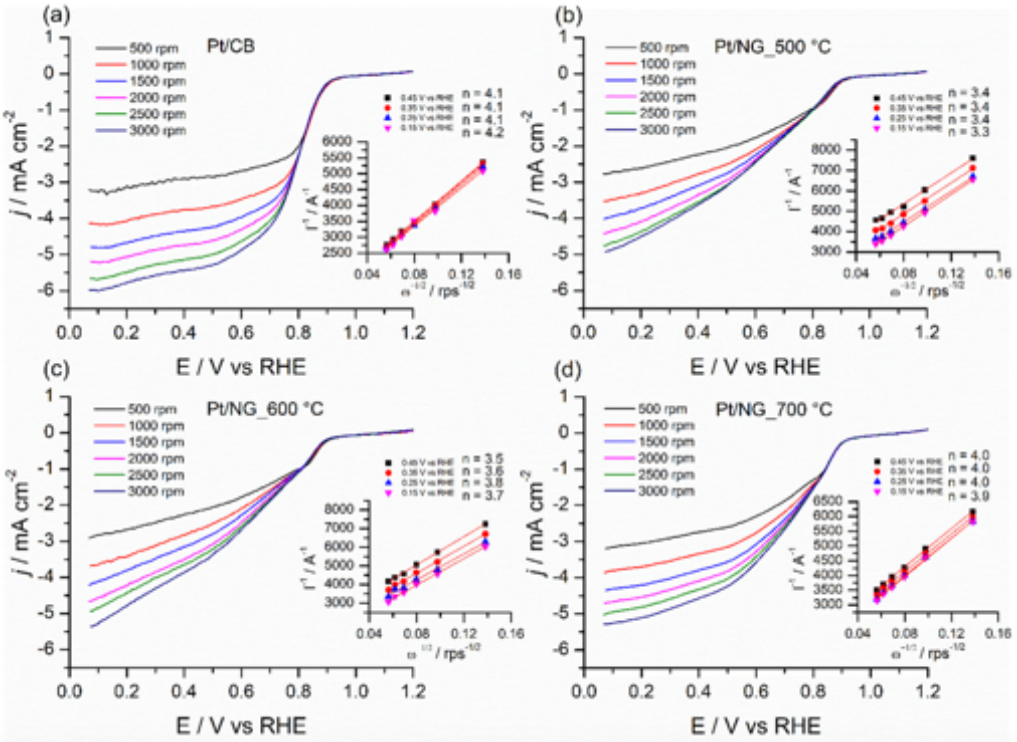

**3) Tamás Varga, Gergő Ballai, Lívia Vásárhelyi, Henrik Haspel, Ákos Kukovecz, Zoltán Kónya: Co4N/nitrogen-doped graphene: A non-noble metal oxygen reduction electrocatalyst for alkaline fuel cells, *Applied Catalysis B: Environmental*, 237 (2018) 826-834.**

We developed a method to realize N-doping and Co4N deposition on graphene flakes. The method is illustrated in the figure below. (T. Varga et al., Appl. Catal. B - Environmental 2018).

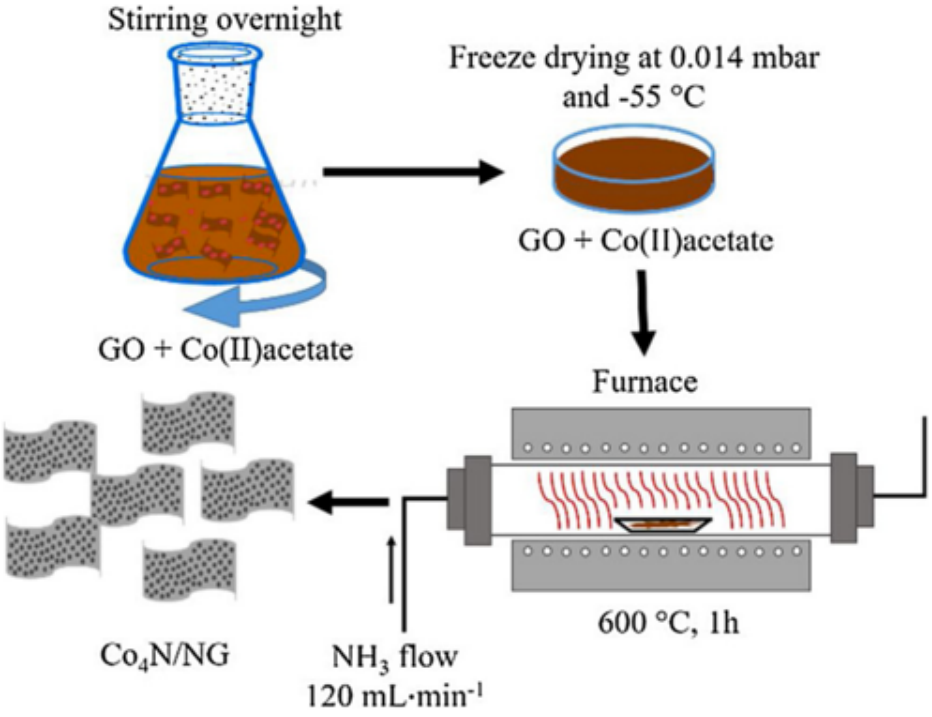


**4) J. Kiss, Á. Kukovecz, Z. Kónya: Beyond Nanoparticles: The Role of Sub-nanosized Metal Species in Heterogeneous Catalysis, Catal. Lett. 149 (2019) 1441-1454.**

Here we have given a perspective overview of the role of sub-nanosized metal species in heterogeneous catalysis. Considering the fact that interfacial electron structure properties have a major effect on both heterogeneous catalysis and electron/hole transport properties, this work has direct relevance for the present project.

Titanate nanostructures are of great interest for catalytic applications because their high surface area and cation exchange capacity create the possibility to achieve high metal dispersion. Ion exchange allows titanate nanostructures to incorporate metal adatoms in their framework. Consequently, the curved layers contain a large amount of defect sites, typically oxygen vacancies and $Ti^{3+}$ centers, which can make them promising photocatalysts, because the defect sites can trap photoelectrons or holes extending the lifetime of the excited state. Due to the large amount of defects, titanate nanotubes (TNT) can stabi- lize sub-nanosized gold clusters, presumably in $Au_{25}$ form. This perspective summarizes the previous results obtained in the photocatalytic transformation of methane in which the size of gold nanoclusters plays an important role. Photocatalytic measurements revealed that methane is active towards photo-oxidation. Methane transforms mainly into hydrogen and, to a lesser extent, to ethane and ethanol. Based on recent additional results, we stress here that gold clusters ($Au_{25}$) may be directly involved in the photo-induced reactions, namely in the direct activation of the methane/$Au_{25}^{\delta+}$ complex during irradiation.

Another new finding is that gold nanoparticles supported on TNT exhibit high catalytic activity in $CO_2$ hydrogenation. Our results revealed fundamental differences in the reaction schemes as the products of the two routes are CO (thermal process) and $CH_4$ (photocatalytic route), indicating the importance of photogenerated electron–hole pairs in the reaction. The presence of gold nanoparticles on the surface has been found to have multiple roles. On the one hand, gold in nano and sub-nano sizes promotes the adsorption and scission of reactants, important for both types of reactions. On the other hand, the gold-support interface forms a rectifying Schottky contact that helps in the separation of photogenerated carriers, thus improving the utilization of electrons and holes in the reduction and oxidation steps, respectively. Furthermore, gold ions ($Au^+$), in the cationic sites of the titanate lattice promote the photocatalytic transformation of formate (which is one of the intermediates), thus advancing the reaction further towards the fully reduced product. The explored reaction schemes may pave the road towards novel catalytic materials that can solve challenges associated with the activation of $CH_4$ and $CO_2$ and thus contribute to green chemistry.

**5) A. Rawal., P.V. Kameswara Rao, V. Kumar, S. Sharma, S. Shukla, D. Sebők, I. Szenti, Á. Kukovecz, Optimal design of absorptive glass mat (AGM) separator with fastest electrolyte uptake using X-ray micro-computed tomography, J. Energ. Stor. 21 (2019) 505-509.**

Here we suggested novel design principles for absorptive glass mat separators based on X-ray micro-computed tomography. The relevance of this work for the present project is that by using microCT to experimentally validate the theoretical model for fibrous materials, it paves the way towards applying the model to similar fibrous structures occurring in other energy-related applications. One evident possible application is the development of electron and/or hole transport layers based on one dimensional nanostructures (e.g. inorganic nanowires) in perovskite based solar cells.

Valve regulated lead acid (VRLA) batteries are traditionally classified on the basis of gel and absorptive glass mat (AGM) separators. To fulfill the desired functions of AGM batteries, a key design feature of the separator relies on the uptake of the electrolyte in shortest transport time. We present a three-dimensional (3D) analytical model to predict the fastest electrolyte uptake in AGM separators based upon the optimal set of fiber and structural parameters. The predictive model has utilized 3D data of fiber orientation in AGM separators, ob- tained via X-ray micro-computed tomography analysis. Such realistic structural information of AGM has assisted in simulating the separators made up of cheaper coarser glass fibers, which was subsequently benchmarked with the experimental samples consisting of finer fibers for attaining the fastest electrolyte uptake. Through theoretical modeling, a design criterion has successfully evolved for the fastest electrolyte uptake by mapping the key effects of the fiber diameter, 3D fiber orientation distribution and porosity of AGM separators. In general, high- density AGM separators comprising of preferentially aligned coarser fibers tend to attain the fastest electrolyte uptake.

The figure below shows (a) a 3D rendered image and (b) 3D fiber orientation distribution of an AGM sample obtained via X-ray microCT analysis.

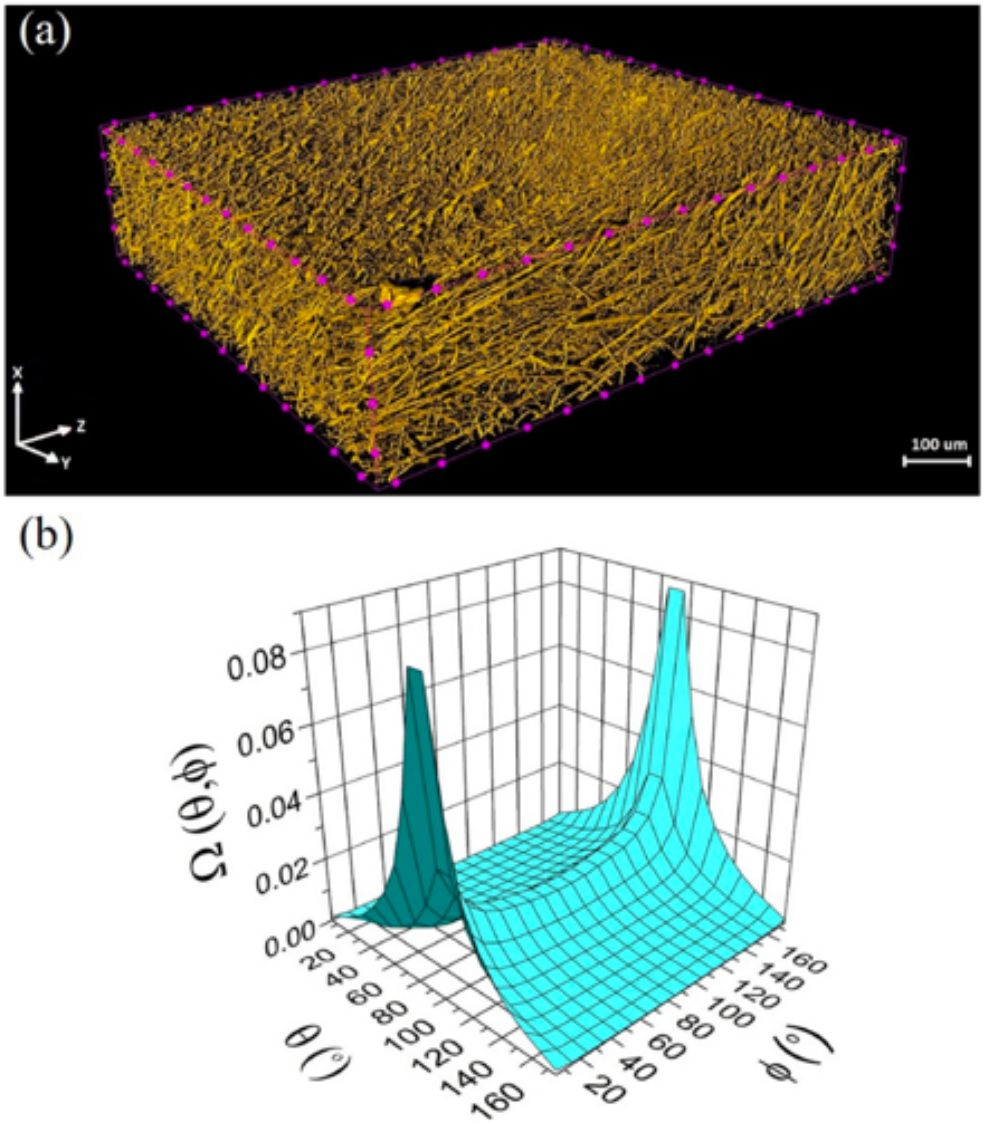


**6) T. Varga, L. Vásárhelyi, G. Ballai, H. Haspel, A. Oszkó, Á. Kukovecz, Z. Kónya, Noble-Metal-Free Iron Nitride/Nitrogen-Doped Graphene Composite for the Oxygen Reduction Reaction, ACS Omega 4 (2019) 130-139.**

This work is directly related to the present project because it reports on the development of the novel nanostructure, an iron nitride/N-doped graphene nanocomposite that could be advantageously applied in the oxygen reduction reaction. It seems possible that such nanocomposites could also be used as electron transfer layers in perovskite solar cells.

Considerable effort has been devoted recently to replace platinum-based catalysts with their non-noble-metal counterparts in the oxygen reduction reaction (ORR) in fuel cells. Nitrogen-doped carbon structures emerged as possible candidates for this role, and their earth-abundant metal- decorated composites showed great promise. Here, we report on the simultaneous formation of nitrogen-doped graphene and iron nitride from the lyophilized mixture of graphene oxide and iron salt by high-temperature annealing in ammonia atmosphere. A mixture of FeN and $Fe_2N$ particles was formed with average particle size increasing from 23.4 to 127.0 nm and iron content ranging from 5 to 50 wt %. The

electrocatalytic oxygen reduction activity was investigated via the rotating disk electrode method in alkaline media. The highest current density of 3.65 mA $cm^{-2}$ at 1500 rpm rotation rate was achieved in the 20 wt % catalyst via the four-electrode reduction pathway, exceeding the activity of both the pristine iron nitride and the undecorated nitrogen-doped graphene. Since our catalysts showed improved methanol tolerance compared to the platinum- based ones, the formed non-noble-metal system offers a viable alternative to the platinum-decorated carbon black (Pt/CB) ORR catalysts in direct methanol fuel cells.

**7) Krisztina Anita Nagy, Ildikó Y. Tóth, Gergő Ballai, Ágnes Timea Varga, Imre Szenti, Dániel Sebők, Judit Kopniczky, BélaHopp, Ákos Kukovecz, Wetting and evaporation on a carbon cloth type gas diffusion layer for passive direct alcohol fuel cells, Journal of Molecular Liquids 304 (2020) 112698**

Gas diffusion layers (GDL) have a crucial importance in passive air breathing direct alcohol fuel cells as they play a pivotal role in governing fuel distribution on the anode side and inpreventing water flooding on the cathode side. We report here a rapid, cost-effective, ex-situ method to study the wettability of GDLs by process fluids. A commercial Teflon® treated carbon cloth featuring a single microporous layer was used, because carbon cloths are anticipated to outperform carbon paper type GDLs at high humidity and high current density. The GDL structure was characterized by SEM, 3D microCT reconstruction, and surface profilometry. Wettability by aqueous alcohol mixtures was investigated by contact angle measurement and infrared thermography. Ethanol containing fuel offered better spreading characteristics than methanol, especially on the microporous side of the GDL. The surface behaviour of water was studied by recording the evaporation profile ofa sessile water droplet using time dependent contact angle measurement and simultaneous weight loss measurement and thermography. The applicability of the Teflon-containing carbon cloth as a GDL was verified by its hydrophobic behaviour and its ability to reject water. We found evidence that the first stage of water evaporation occurs in constant contact angle mode, then a wetting mode transition takes place at approx. 0.65 relative evaporation time and the evaporation proceeds in constant contact radius mode.

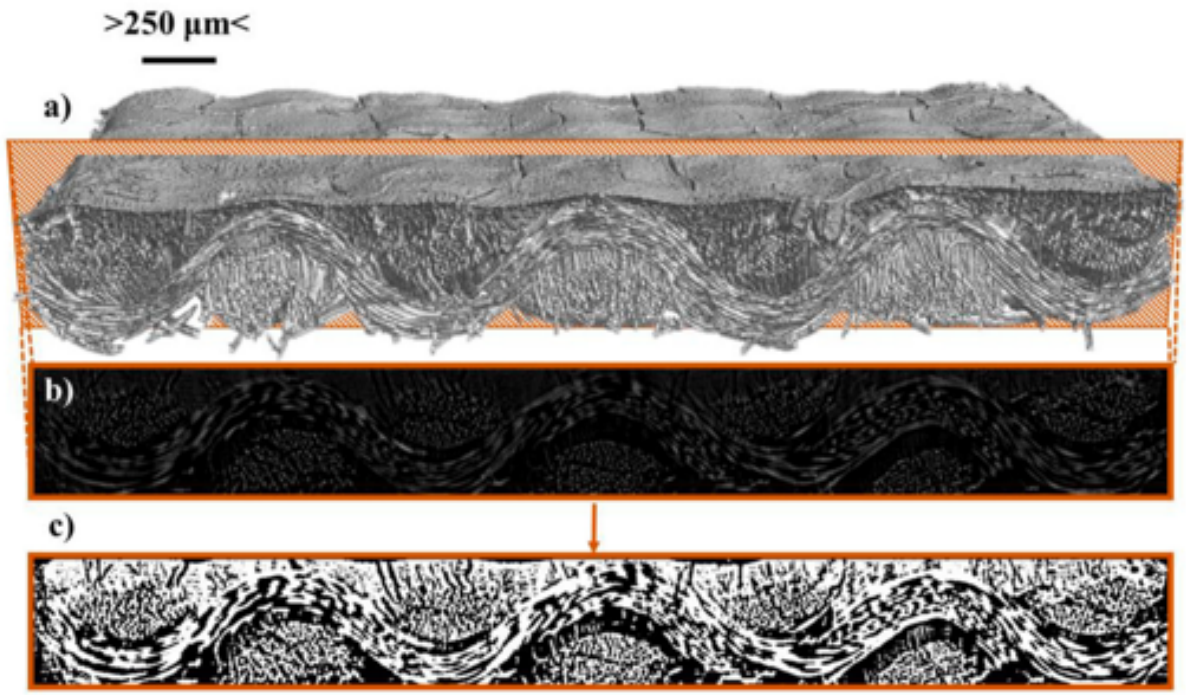

Cross-sectional CT images from the carbon cloth: a representative volume rendered 3D picture (a), a slice image (b) from the 3D picture and a segmented (black and white) image (c) from the slice.

The relevance of this work for the CLEARPV project is in uncovering new knowledge about the structural and wetting properties of a typical cloth material used heavily by the energy industry. Since the GDL is made of electrically conductive carbon and it is flexible, it is a potentially useful support layer that can be utilized in wearable or building-integrated photovoltaics.

**8) L. Vásárhelyi, Z. Kónya, Á. Kukovecz, R. Vajtai, Microcomputed tomographyebased characterization of advanced materials: a review, Materials Today Advances 8 (2020) 100084**

Micro-computed tomography (CT) is an X-ray tomography technique with (sub)micron resolution, typically using an X-ray tube with cone-beam geometry as a source and a rotating sample holder. While conventional CT maintained a strong position in life science and low-resolution high-energy CT became widespread in industrial quality control, micro-CT has enjoyed a boost in interest from the materials science research community in the past decade. The key reasons behind this are the versatile, non- destructive nature of micro-CT as a characterization method offering also in situ and in operando possibilities and the fact that micro-CT has become indispensable in developing and verifying computational material models as well. The goal of this mini review was to give a concise introduction of the method to newcomers and showcase a few impressive recent results that can help in devising even more innovative future uses of micro-CT. After a brief overview of alternative three-dimensional imaging techniques, we reviewed the basics of micro-CT covering important concepts such as resolution, magnification, and the Hounsfield unit. The second part of the article summarizes characteristic materials science micro-CT applications in bioinspired

materials, structural materials, porous natural materials, energy storage, energy conversion, and filtration.

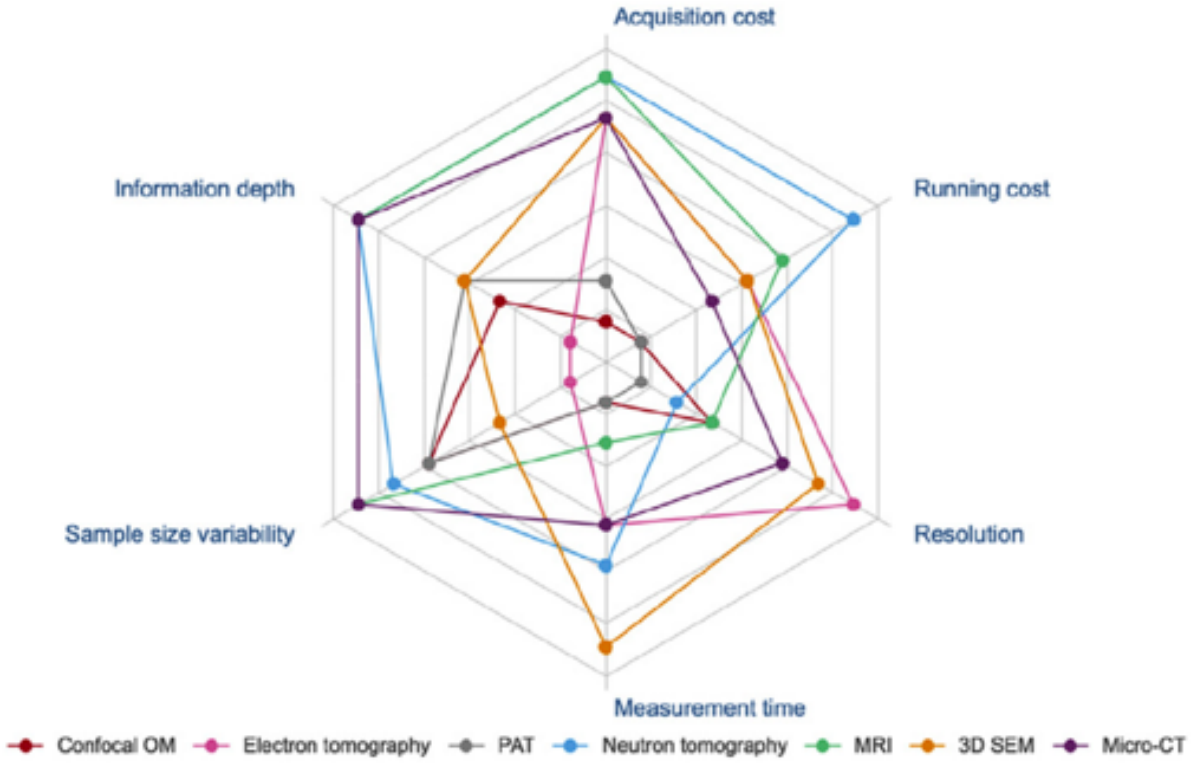


Radar chart of the comparison of 3D imaging modalities. Axes are scaled in relative arbitrary units to facilitate qualitative comparison.

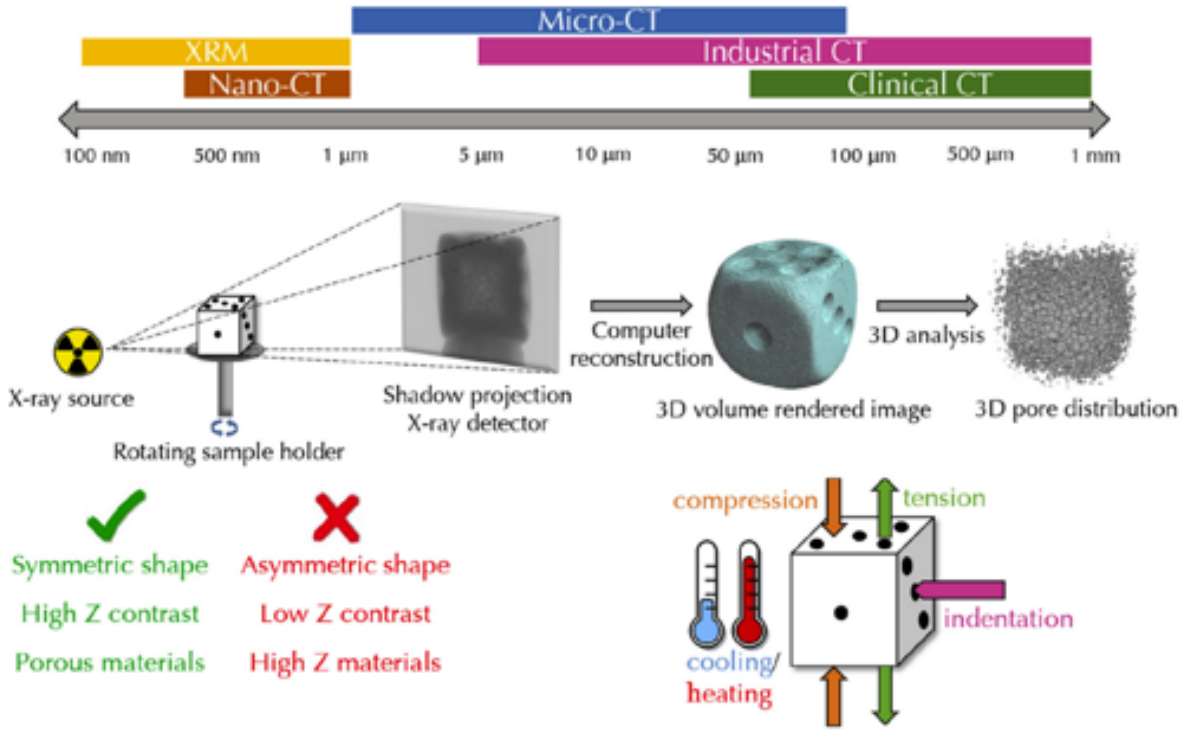

A micro-CT cheat sheet prepared using actual images of a commercial dice recorded in the Hungarian partner laboratory. In situ measurement possibilities are limited only by innovativeness in measurement cell design. Thus, custom-made equipment for, for example, electrical testing, catalytic reactions studying wetting/wicking phenomena is also used. CT, computed tomography.

The relevance of this work for the CLEARPV project is that micro-CT is a very promising technique for the characterization of assembled photovoltaic modules, especially with respect to manufacturing failures, inhomogeneites, cracks in intermittent layers etc. In the framework of the CLEARPV project TNO and the Hungarian partner have collaborated in developing the micro-CT based analytics of perovskite thin film solar cells. Unfortunately, the resolution of the currently available Bruker SkyScan 2211 unit was insufficient to provide meaningful images of the active perovskite layer. However, this research line has a lot of potential and we will be continuously developing it even after the conclusion of the CLEARPV project.

**9) Viktor Havasi, David Tatrai, Gabor Szabo, Erika Varga, Andras Erdohelyi, Gyorgy Sipos, Zoltan Konya, Akos Kukovecz, On the effects of milling and thermal regeneration on the luminescence properties of Eu2+ and Dy3+ doped strontium aluminate phosphors, Journal of Luminescence 219 (2020) 116917**

This paper reported on the comparison of luminescence, particle size and crystallinity reduction of SrAl2O4: Eu2+, Dy3+ (SA2) and Sr4Al14O25: Eu2+, Dy3+ (SA14) phosphors by ball milling. In addition, the regeneration possibilities of rare earth metal doped strontium aluminate phosphors (SAEDs) were investigated. The crystallinity degradation and particle size reduction were characterized by powder X-ray diffraction, and scanning electron microscopy (SEM) techniques respectively. Afterglow (AG), photo- (PL) and thermoluminescent (TL) properties of SAEDs were followed in parallel. The trap level shifts during the degradation and regeneration process were calculated from the TL data. The oxidation and reduction of Eu2+/3+ luminescence centre was followed by X-ray photoelectron spectroscopy (XPS). Luminescence degradation became significant after 2 μm avg. particle diameter reached, for both SAEDs. Considerable differences were found in their stress durabilities. The SA2 and SA14 characteristics are largely influenced by the details of the mechanical energy investment method, in reached crystallinity, particle diameter, and the Eu2+/3+ state, besides the total amount of energy transferred. The reversibility of the Eu2+/3+ ratio, PL and afterglow performance of the milled phosphors could be restored to some extent, by similar to synthesis annealing. The SA14 and SA2 phosphors responded differently to the regeneration process.

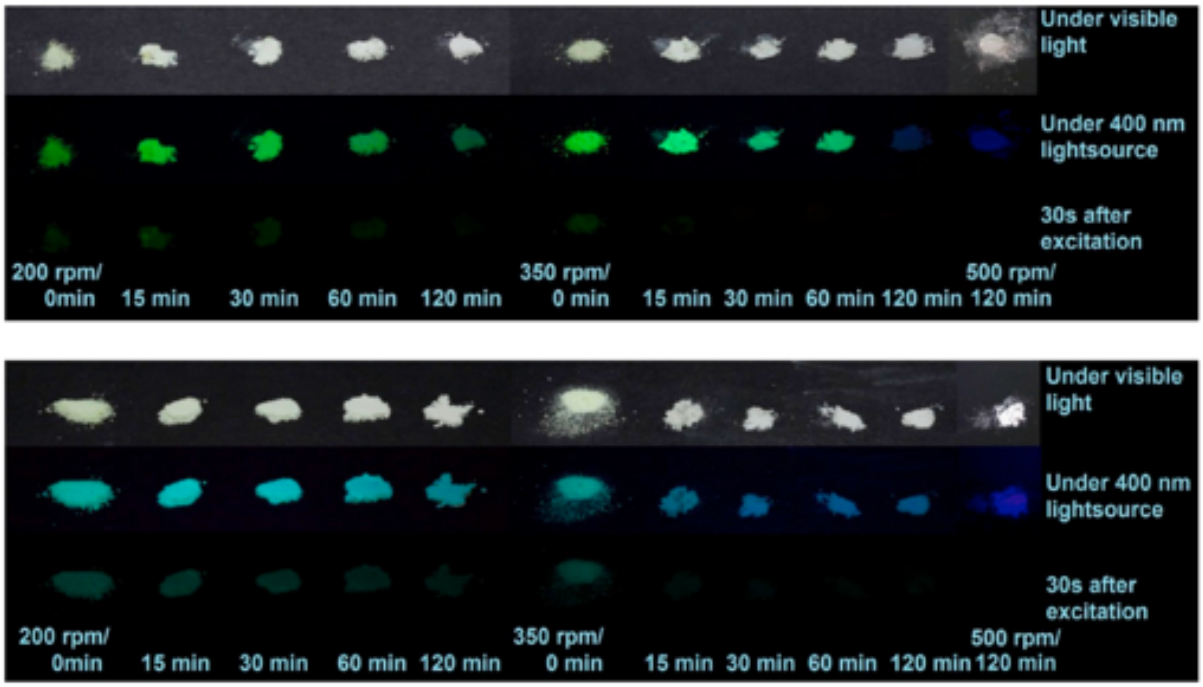


Optical images of SA2 (top) and SA14 (bottom) phosphors milled and illuminated under various conditions.

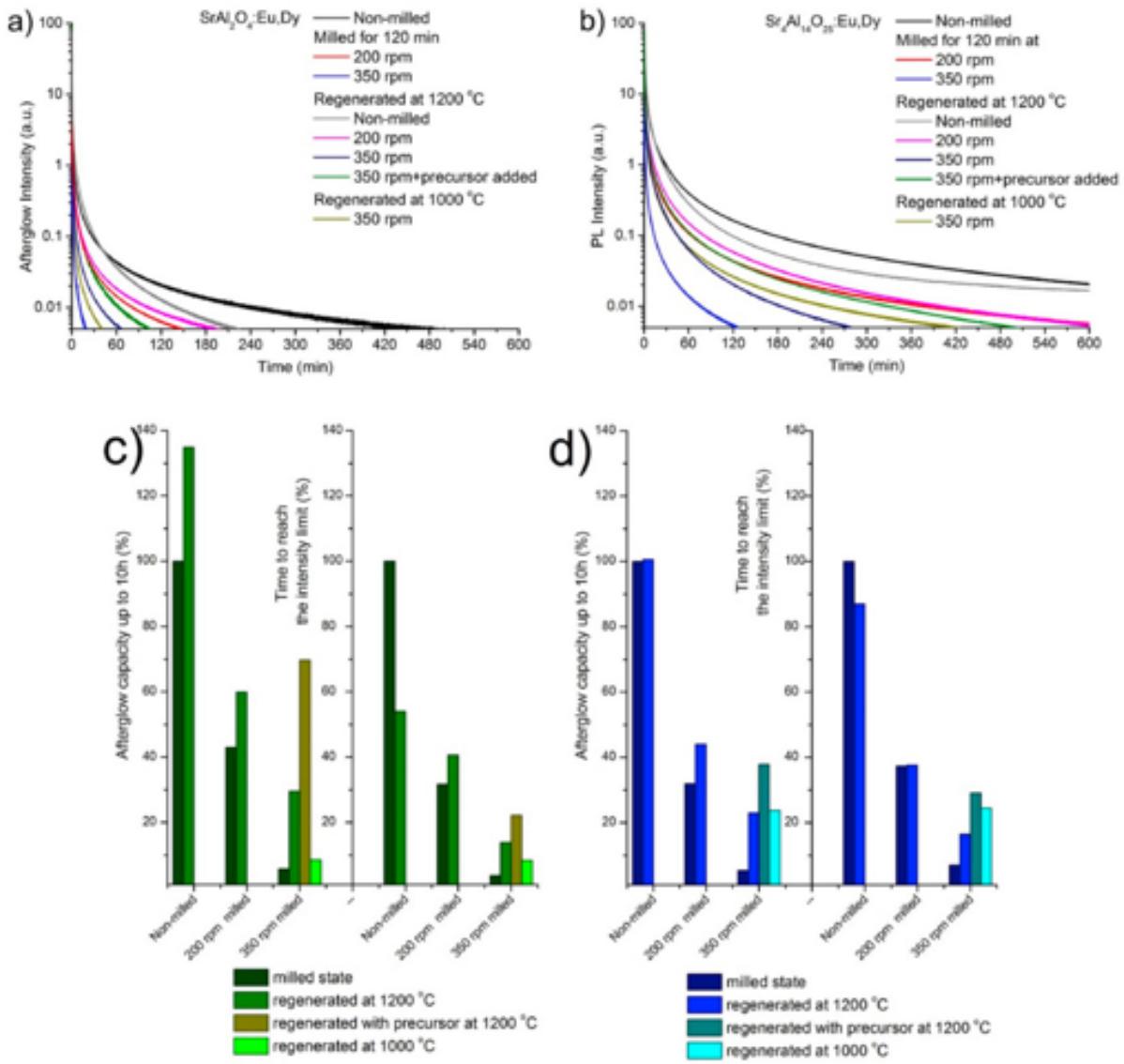


Afterglow curves of milled and regenerated SA2 (a) and SA14 (b) phosphors. Overall integrated area as afterglow capacities of milled SA2 and SA14 phosphors (c) and the time needed to reach the arbitrary 0.005% of the initial intensity of the non-milled sample (d).

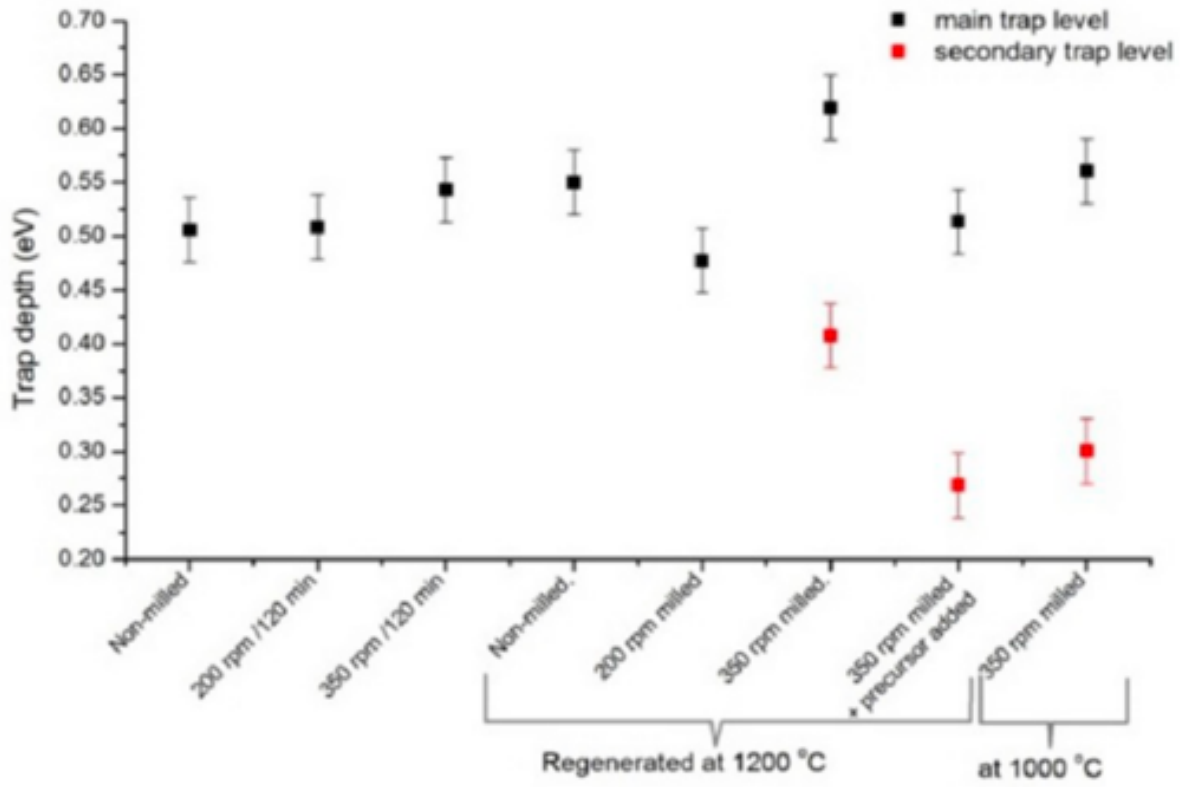


The relevance of this work for the CLEARPV project is direct and evident. It is the primary objective of the Szeged partner in the network to develop new semiconductor oxide materials with advanced and tunable optical properties, and study their behavior upon size reduction. This was the main focus of the published work where we have demonstrated important differences in the milling-induced function loss and thermal recovery of strontium-aluminate phosphors. It is worth noting that such phosphors are intensely researched in multiple photovoltaic applications today.

**10) Viktor Havasi, György Sipos, Zoltán Kónya, Ákos Kukovecz, Luminescence and color properties of Ho3+ co-activated Sr4Al14O25: Eu2+, Dy3+ phosphors, Journal of Luminescence 220 (2020) 116980**

We report on the photoluminescence properties of Sr4Al14O25:Eu2+,Dy3+ (SAED) phosphors modified by adding Ho3+ in excess and partially substituting Dy3þ with Ho3+ (SAEDHs). Samples were produced using an established solid-state synthesis method known to consistently yield long-persistent afterglow phoshors. Substitutions were performed in stoichiometrically modified host lattices (Al/Sr ¼ 3.2, 3.5, 3.7). Partially substituting Dy3+ with Ho3þ resulted in a remarkable increase in photoluminescence (PL) intensity, Ho3+ co-doping caused a shift in the main emission peaks between 494 and 497 nm and introduced new peaks as well. Important from the security application point of view, the PL intensity was significantly improved under both purple (400 nm) and blue (445 nm) illumination. Color shift of the powders from green to a yellowish and pale pink shade resulted from the Ho3þ addition. Afterglow (AG) properties and thermoluminescence (TL) response decreased non-gradually as Dy3+ was substituted by Ho3þ, due to possible charge transfer effects caused by Ho3+. AG and TL properties remained more intact in the presence of Ho3+ when the Al/Sr ratio differed

from the ideal 3.5 ratio. Rearrangements of trap energy levels, and energy transfer induced by Ho3+ co-doping were analysed by TL. Dy3+/ Ho3+ co-dopants and Al/Sr stoichiometric ratios asymmetrically influenced the trapping/detrapping and energy transfer processes of the SAEDH phosphors. The developed new materials meet the general characteristics of long-persistent phosphors: charging by sunlight, efficient light conversion, chemical stability, all-night afterglow observable by the human eye.

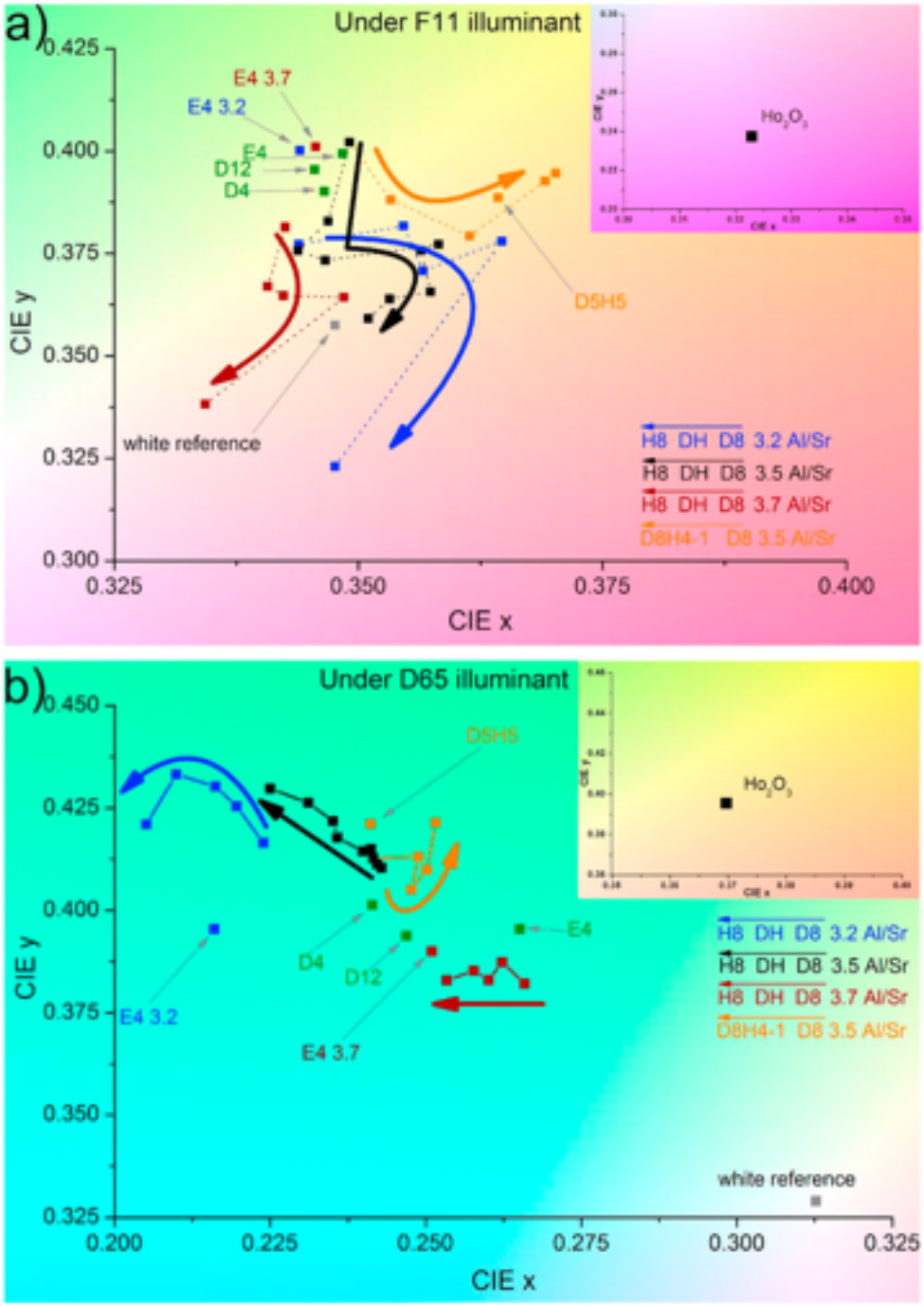

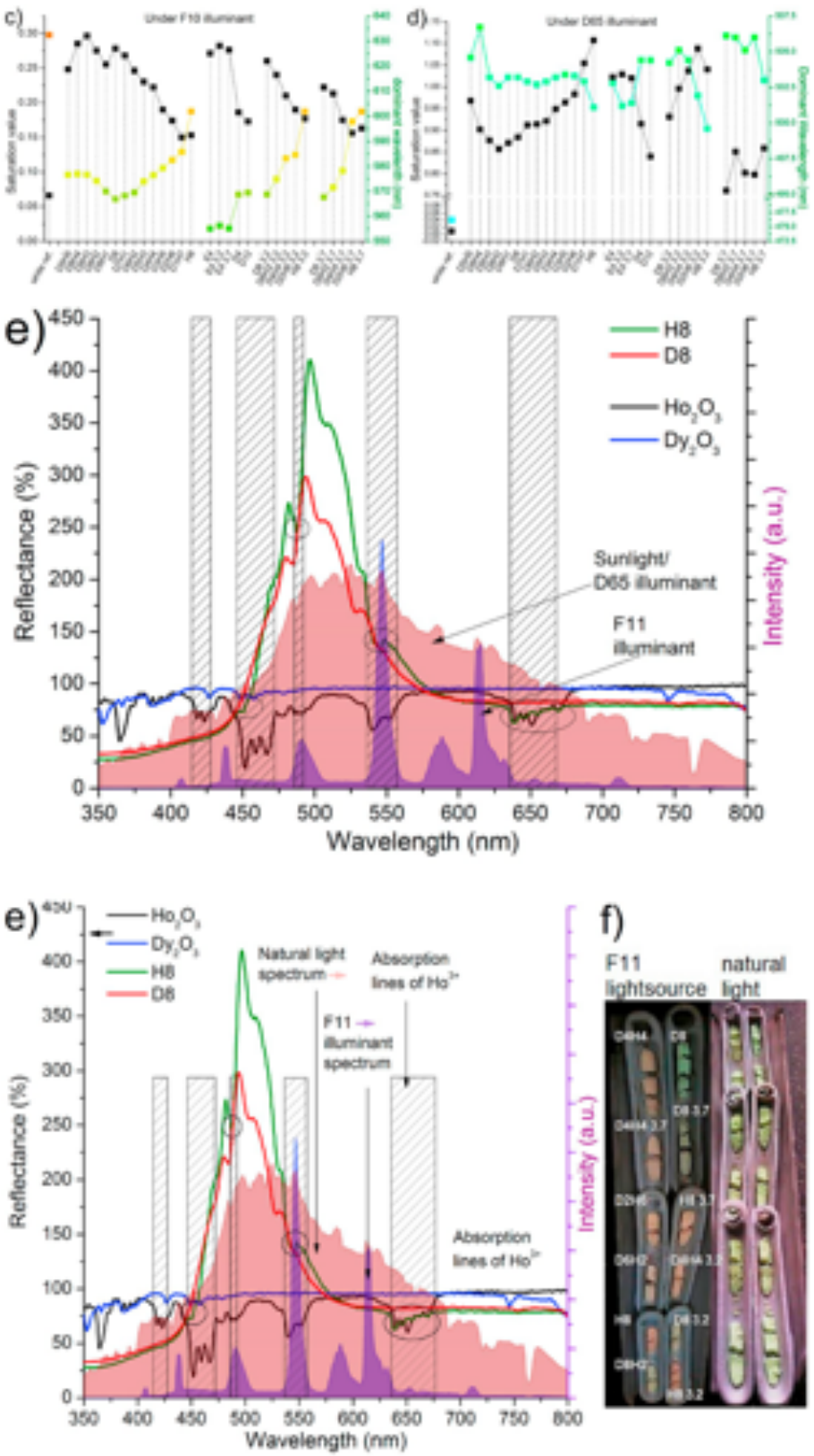


Color coordinates of SAEDHs in the CIE xy color space under F11 illuminant (a), and under D65 illuminant (b). Embedded pictures show the color coordinates of Ho2O3. Dominant wavelength and saturation values of the SAEDHs in the CIE LUV color space, under F11 (c) and D65 (d) illumi- nants. Comparison of precursors, phosphors, and illuminant spectra (e). Photos of as prepared phosphors under fluorescent (left) and natural (right) light (f).

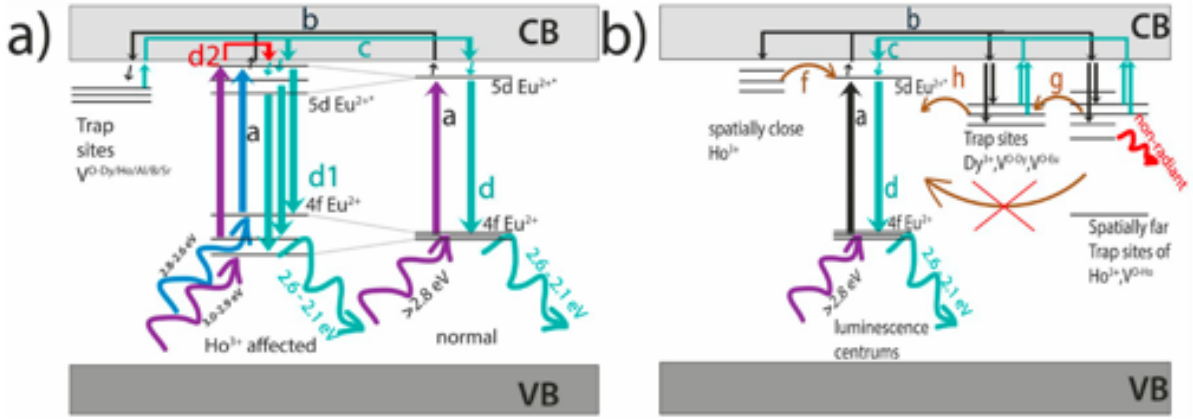


Suggested mechanism for a) the sensitizing effect by Ho3+ co-dopant in SAEDHs, and on Eu2+ luminescence centrum b) Possible charge transfers and anomalous trapping/re-trapping phenomena induced by Ho3+ co-dopant. Processes (a, b, c, d) represent the TSC based excitation, trapping, re-trapping and relaxation with photon radiation process, respectively. The (e, f) processes represent energy transfers via NTSC ways between lanthanides and other trap-sites.

The relevance of this work for the CLEARPV project is direct and evident. It is the primary objective of the Szeged partner in the network to develop new semiconductor oxide materials with advanced and tunable optical properties, and study their behavior upon size reduction. This was the main focus of the published work where we have systematically studied the effects of Ho3+ co-activation on SA14 strontium-aluminate phosphors. Such phosphors are currently intensively research in solar cell applications including perovskite based solutions.

**11) Meng Zheng, Francesco Lamberti, Lorenzo Franco, Elisabetta Collini, Ilaria Fortunati, Gregorio Bottaro, Giorgia Daniel, Roberto Sorrentino, Alessandro Minotto, Akos Kukovecz, Enzo Menna, Simone Silvestrini, Christian Durante, Franco Cacialli, Gaudenzio Meneghesso, Michele Maggini, Teresa Gatti, A film-forming graphene/diketopyrrolopyrrole covalent hybrid with far-red optical features: Evidence of photo-stability, Synthetic Metals 258 (2019) 116201**

A dianiline derivative of a symmetric donor-acceptor-donor diketopyrrolopyrrole-based dye is employed for the two-sided covalent functionalization of liquid exfoliated few layers graphene flakes, through a direct arylation reaction. The resulting nanohybrid features the properties of a polymeric species, being solution-processed into homogeneous thin films, featuring a pronounced red-shift of the main absorption band with respect to the model dye unit and energy levels comparable to those of common diketopyrrolopyrrole-based polymers. A good electrical conductivity and the absence of radical signals generated after intense white light illumination, as probed through electron paramagnetic resonance, suggest a possible future application of this composite material in the field of photoprotective, antistatic layers with tunable colors.

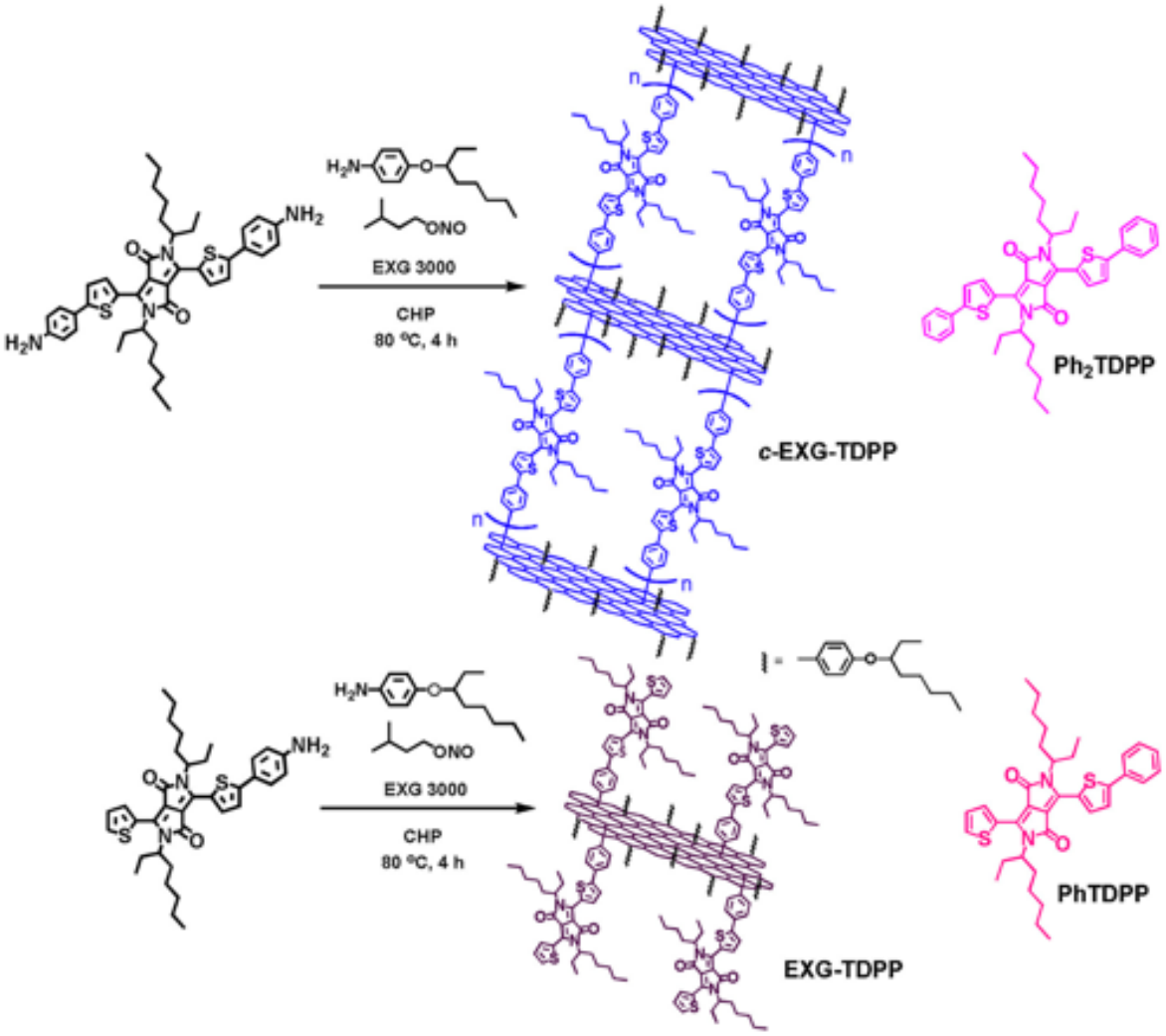


Synthesis of the cross-linked graphene-diketopyrrolopyrrole hybrid (c-EXG-TDPP, blue) and of the reference material lacking cross-linking (EXG-TDPP, purple). Both the graphene-diketopyrrolopyrrole hybrids are obtained through in-situ direct arylation starting from EXG 3000 and the corresponding di- and monoaniline derivatives. The materials are co-functionalized with 4-[(2-ethyl)hexyloxy]phenyl moieties to improve the solubility. The structure of the two corresponding reference small molecules, Ph2TDPP and PhTDPP, is also reported for the sake of clarity.

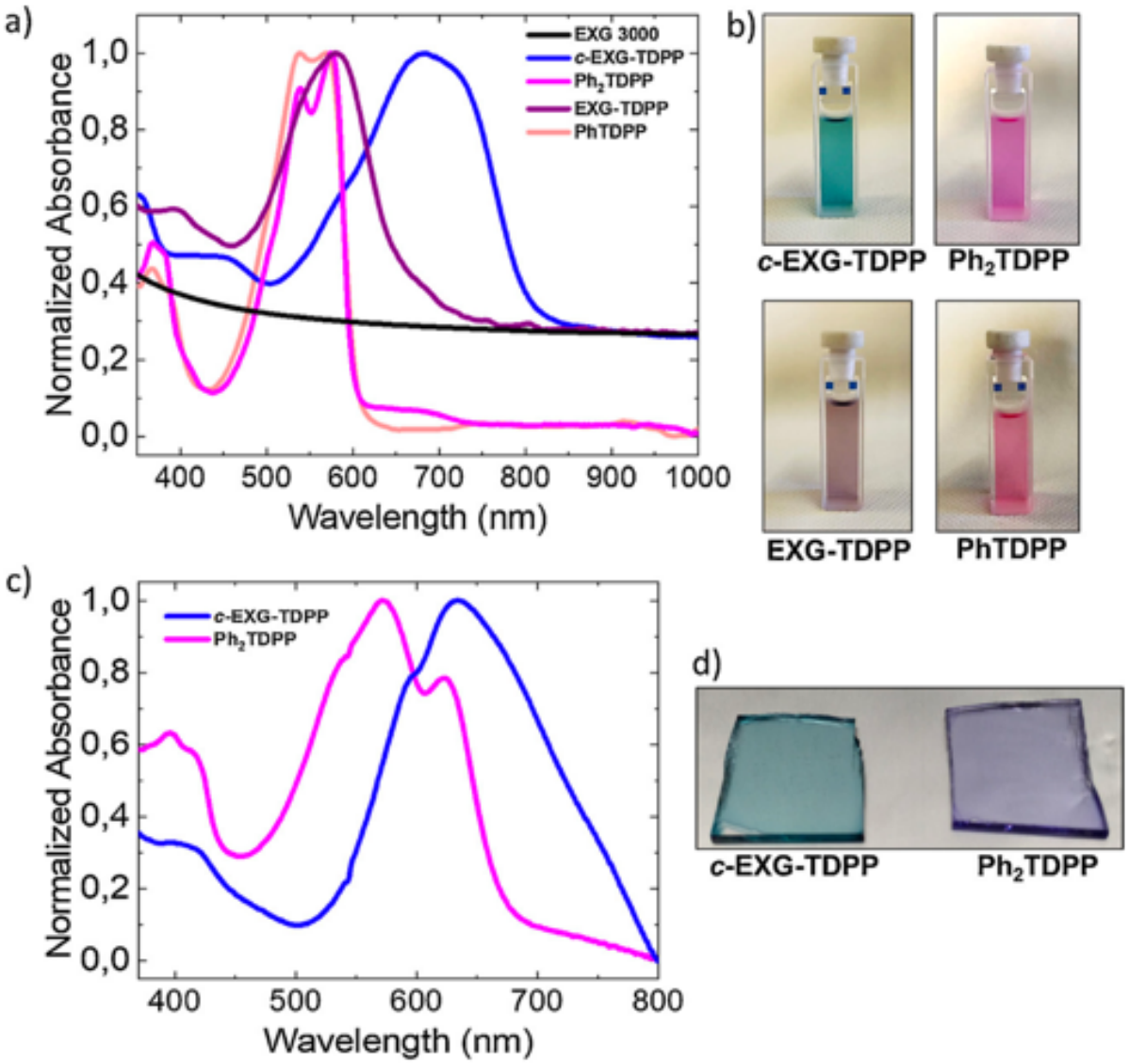


Optical characterization of the graphene-diketo- pyrrolopyrrole hybrids compared to reference small molecules and pristine EXG 3000. a) Normalized UV–vis-NIR absorption spectra of the hybrids and of the corresponding reference small molecules in DMF solutions. The spectrum of EXG 3000 is also reported for comparison (a drop of the ink in CHP was diluted with DMF to record the spectrum). b) Photos showing the appearance of the DMF solutions of the graphene-diketopyrrolopyrrole hybrids and of their reference small molecules. c) Normalized UV–vis absorption spectra of the cross-linked graphene-diketopyrrolo- pyrrole hybrid and of its reference small molecules in spin- coated thin films obtained from toluene solutions on glass slides. The pictures of these films are reported in d).

The relevance of this work for the CLEARPV project is direct and evident. This excursion towards thin-forming organic semiconductors was undertaken to supplement the NTU (Taiwan) efforts and investigate if the integration of graphene flakes with the organic semiconductor material is feasible for tuning the optical and electrical properties of the layer. The results were compared with those obtained at NTU and the future research directions of the CLEARPV project were determined accordingly.

**12) Mucsi, László Óvári, János Kiss, Zsolt Fogarassy, Béla Pécz, Ákos Kukovecz, Zoltán Kónya, Ambient pressure CO2 hydrogenation over a cobalt/manganese-oxide nanostructured interface: A combined in situ and ex situ study, Journal of Catalysis 386 (2020) 70–80**

We report on a cobalt/manganese-oxide interface catalyst with outstanding activity and selectivity towards methane even at high temperatures and ambient pressure in CO2 hydrogenation. The catalyst was formed from a MnCo2O4-based spinel structure during the oxidative-reductive pretreatment process just before the catalytic tests. Several Mn-, Fe- and Ni-containing cobaltite spinel and reverse spinel structures were tested to find the best overall performer. The reusable MnCo2O4-based structure featured a CO2 consumption rate of ~8500 nmol*g-1*s-1. Even though methane is not the thermodynamically favoured product, it was produced with ~80% and ~50% selectivity at ambient pressure at 673 K and 823 K, respectively. This unexpected finding is linked to the presence of a unique nanostructured Co/ Mn(II)O catalyst with a surface composition of Mn3.3Co2.0O4.7 formed after the pretreatment activation step. Over this phase, the reduction of CO2 progresses through bridge bonded formate located at the Co/Mn2+ interface and this is mostly responsible for high temperature methane formation. This hypoth- esis is proven here by the reported combination of ex-situ XRD, TPR, HRTEM-ED, HAADF-EDX and in-situ NAP-XPS and DRIFTS techniques.

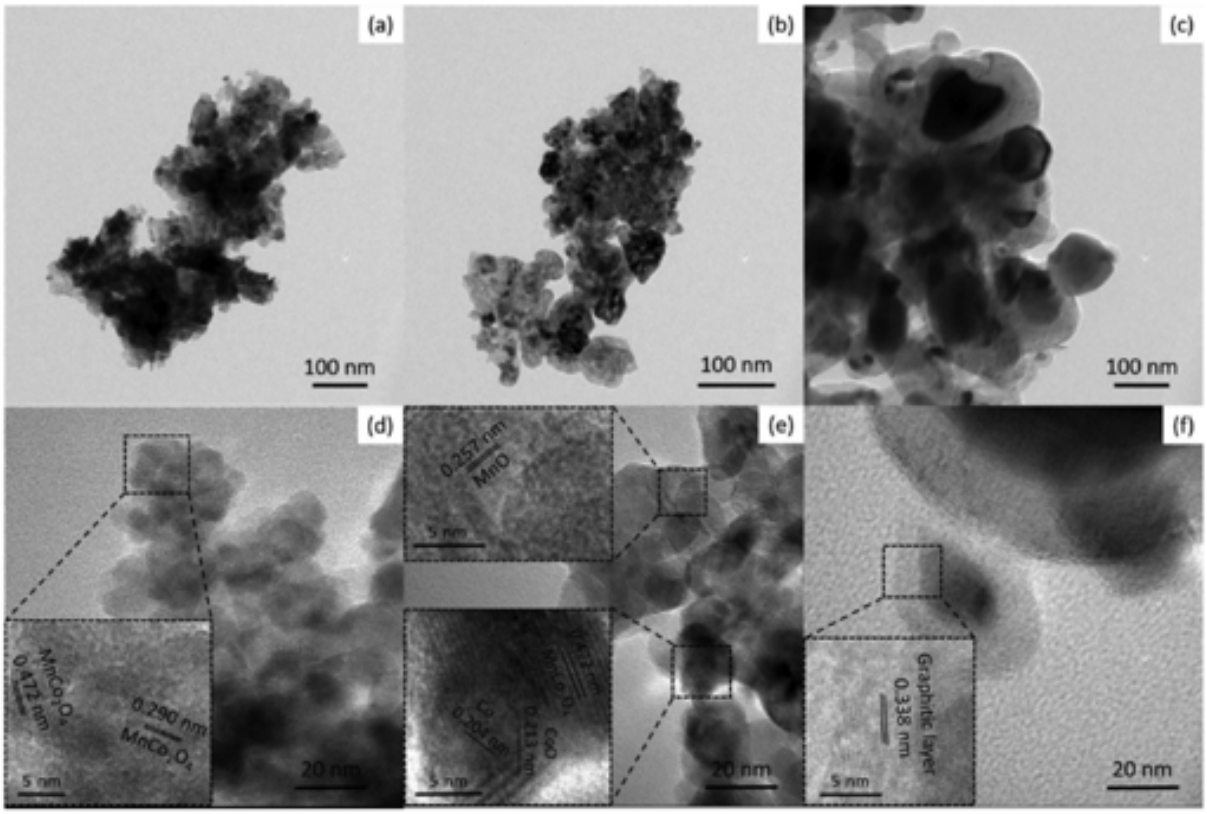


TEM images of MnCo2O4 (a, d) as-synthetized, (b, e) after the reduction step (300 °CO2 for 1 h followed by 300 °CH2, 1 h) and (c, f) after CO2 hydrogenation 523 – 823 K.

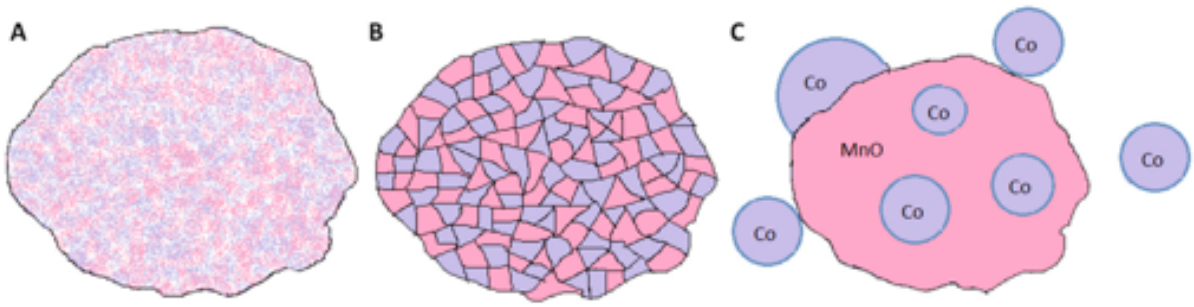


Schematic view of the transformation of MnCo2O4 spinel structure (A) to the Co/MnO nanostructure (C) through the mixed oxide phase (B).

The relevance of this work for the CLEARPV project is that it took the classical approach in synthesizing a mixed oxide semiconductor material. The functionality of this new Co/Mn-oxide was verified in a simple heterogeneous catalytic experiment because the 2020 COVID pandemic has limited our ability to move personnel within the consortium for e.g. testing the applicability of the new material as a transfer layer at TNO's laboratories. Nevertheless, the catalytic results are promising enough to justify a new transfer layer test round in the near future.

**4. Other results**

4.1

The secondment of Levente Sánta at TNO Eindhoven has generated a large set of results on semiconductor oxide layers with potential use in perovskite solar cells. However, these results remain the property of TNO and we are not allowed to disclose them publicly.

4.2

**13) Elvin Y. Malikov, Melek C. Altay, Oktay H. Akperov, Mustafa B. Muradov, Goncha M. Eyvazova, Ákos Kukovecz, Zoltán Kónya: Effect of sonication time on the synthesis of the CdS nanoparticle based multiwall carbon nanotube – maleic anhydride – 1-octene nanocomposites, *Fullerenes, Nanotubes and Carbon Nanostructures*, 26 (2018) 255-262.**

Here, we explored the synthesis of a polymer-based nanocomposite material. This work also acknowledged the K126065 project because of input received from the project in carbon nanomaterial characterization, however, these results are less likely to find direct applications in the CLEARPV project.